Development of a generalized slenderness-based resistance method for the design of high-strength steel hollow section beam-columns

Andrea Toffolon[1], Andreas Taras [2]

Abstract

The significant increase in the use of high-strength steel has led to a renewed interest in the strength and stability design criteria for hollow sections, owing to the fact that the majority of the resulting cross-sections and beam-columns are to be classified as slender. This paper illustrates a novel approach for the design of slender hollow section members loaded in compression and general bending about both main axes. It introduces a "Generalized Slenderness-based Resistance Method" (GSRM), which was developed over the course of an extensive, multinational and EU-funded research project – HOLLOSSTAB (2016-2019). The GSRM further generalizes the advanced cross-sectional definitions of local and global slenderness used in established strength design methods such as the Direct Strength Method, the Continuous Strength Method and the Overall Interaction Concept, leading to a definition of slenderness that accounts for the overall load case as well as for the elastic buckling strength. This generalized definition of slenderness is used as the basis for the derivation of new design formulae and calibration coefficients for the studied cases, which very closely follow the underlying mechanics while remaining easily handleable. The presented study also includes an analysis of the underlying level of reliability of the GSRM and a representation of its advantages over conventional design methods for slender hollow-section beam-columns. The result of the HOLLOSSTAB project is thus a set of novel design formulae that can be used in combination with bespoke software tools to efficiently and safely determine the ultimate strength of high-strength steel hollow sections.

1 Introduction

Current design standards often provide insufficient accuracy and economy for the design of hollow structural sections (HSS) at a cross-section level – where local buckling effects are prominent – and at a global level, when column-like flexural buckling occurs. The background of the American (AISC) design rules can be found in the work of *Bjorhovde, R. (1972, 1992)* and more recently *Galambos, T. V. (1998)* and *Ziemian, R. D. (2010)*. Cross-sections are divided into categories and the design curve is defined by the squash load in the very stocky range, by a knock-down factor with respect to the Euler load in the slender range, and a transitional function in the intermediate

---
[1] Graduate Research Assistant, Bundeswehr University Munich, andrea.toffolon@unibw.de
[2] Professor – Steel and Composite Structures, ETH Zurich, Institute of Structural Engineering, ataras@ethz.ch

range. The approach and framework of the European standards (Eurocodes), on the other hand, is based primarily on the formulation of various column buckling curves and, for beam-columns, on the application of an interaction formulation that takes the column resistance as a starting point.. The rules for columns in *Eurocode 3: part 1-1* (2018) are based on the work *of Rondal et Maquoi (1979),* whose formulation makes use of the concepts first developed by *Ayrton and Perry* (1886). The formulation is restricted to cases with pure external compression, but accounts for bending moments that develop in imperfect columns in a rational, mechanically-based manner.

One of the objectives of the HOLLOSSTAB project was to derive specific rules for more general load cases in hollow section beam-columns. Thereby, a new method – more general than the current European and North-American design rules – was developed, the so-called "Generalized Slenderness-based Resistance Method" (GSRM). This method further generalizes the advanced cross-sectional definitions of local slenderness used in established strength design methods such as the Direct Strength Method, applying it also to global buckling problems under arbitrary compression and bending loading. While the GSRM design rules for the cross-section resistance are already described in *Toffolon and Taras (2019a and 2019b)*, the current paper focuses on the rules for global buckling. The following sections examine the derivation of design rules for beam-columns against global buckling, starting with a review of the design rules found in the literature and adapted to fit into the Eurocode 3 framework. Then, the new GSRM beam-column design proposal is derived from the previously shown formulations. This derivation is based on second-order theory and basic structural mechanics. A number of calibration factors are introduced, which help to adapt the mechanically derived formulation to better describe the real, elasto-plastic non-linear behavior as observed in physical and numerical tests. Finally, a comparison between the new GSRM rules and the current AISC and EC3 design rules is made, thus validating the newly developed formulation.

2 Ayrton-Perry formulation and Eurocode 3 design rule for columns

As stated above, the original formula to describe the behavior of columns in flexural (global) buckling was first described by *Ayrton and Perry* in 1886. This approach – first employed for a practical case by *Robertson (1925)* – proposes to introduce an equivalent imperfection of sinusoidal shape and amplitude e_0 into a second-order analysis and stress design of a pin-ended model column, and to use this imperfection amplitude as a calibration factor to describe the strength of real columns, as observed e.g. in tests. Ayrton and Perry thus derived their formulation from the elastic buckling amplification factor for a pin-ended column under pure compression with an initial imperfection e_0, leading to the total deflection

$$w = \delta + e_0 = \frac{e_0}{1 - N_b/N_{cr}} \tag{1}$$

where:
δ is the member deflection due to the applied load from the base state
w is the total deflection
N_b is the applied load, which finally leads to column failure.
N_{cr} is the axial force at the first bifurcation point, or "Euler load".

2

Crucially, in the Ayrton-Perry approach a linear cross-sectional failure criterion is introduced, i.e. a linear interaction surface for compression forces and moments is used. At failure, this leads to the following equation:

$$\frac{N_b}{Af_y} + \frac{N_b e_0}{W_y f_y} \cdot \frac{1}{1 - {N_b}/{N_{cr}}} = 1.0 \tag{2}$$

where:
A is the cross-section area.
W_y the cross-section modulus for bending about the y-axis.
f_y is the yield stress.

Current design standards such as the Eurocode use a reduction factor of the cross-sectional plastic resistance in order to define the member strength, and they plot it as a function of the member slenderness. The following variables may thus be introduced:

$$\chi_y = \frac{N_b}{Af_y} \tag{3}$$

$$\bar{\lambda}_y = \sqrt{\frac{Af_y}{N_{cr,y}}} \tag{4}$$

$$\eta_{imp} = \frac{Ae_0}{W_y} \tag{5}$$

where χ_y and $\bar{\lambda}_y$ are, respectively, the knock-down factor and normalized slenderness for buckling about the y-axis, and η_{imp} is a normalization of e_0 by the section core width. These definitions bring the above limit-state equation to the following quadratic format:

$$\chi_y + \eta_{imp} \cdot \frac{\chi_y}{1 - \chi_y \bar{\lambda}_y^2} = 1.0 \tag{6}$$

Which may be solved, leading to the well-known solution:

$$\chi_y = \frac{1}{\Phi + \sqrt{\Phi^2 - \bar{\lambda}_y^2}} \tag{7}$$

with
$$\Phi = 0.5 \cdot \left(1 + \eta_{imp} + \bar{\lambda}_y^2\right) \tag{8}$$

In Eurocode 3, following Ayrton and Perry's original idea, the still-general term η_{imp} is replaced by a formula that makes this imperfection a function of slenderness, of a plateau value to account for stocky columns not failing before the squash load, and of a calibration factor α which accounts for residual stresses and production differences, here denoted as α_{EC3}:

$$\eta_{imp} = \alpha_{EC3}\left(\bar{\lambda}_y - 0.2\right) \tag{9}$$
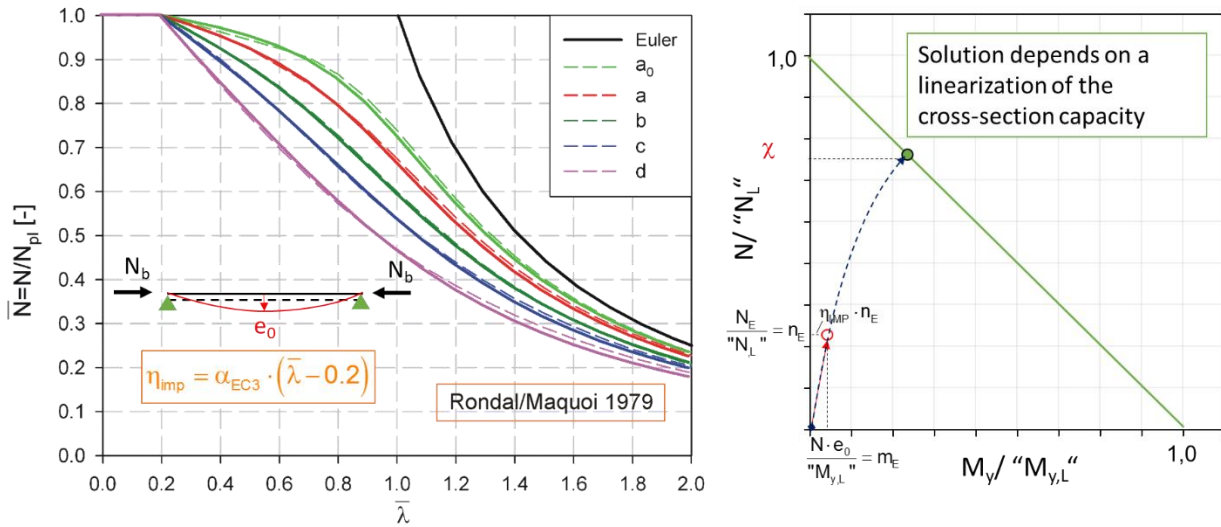
Fig. 1. On the left the parameters η_{imp} from the EC3 formulation and the EC3 buckling curves are represented in the χ - $\bar{\lambda}_y$ plot. On the right a representation of the χ factor in the Ayrton-Perry formulation plotted in the m-n diagram.

Five different values of α_{EC3}, and thus the five well-known "European buckling curves" (a$_0$ to d), exist in Eurocode 3. The α_{EC3} values are given in Table 1 .

Table 1. EN 1993-1-1. Imperfection factors for the determination of the buckling curve.

Buckling curve	a$_0$	a	b	c	d
Imperfection factor α	0.13	0.21	0.34	0.49	0.76

The left-hand side of Fig. 1 shows the resulting European column buckling curves. As can be seen, the calibration to the current EC3 rules, originally performed by *Rondal et Maquoi (1979)*, matches the previously-established, experimental ECCS buckling curves quite accurately across all slenderness ranges. In the right-side plot in Fig. 1, the underlying principle of the Ayrton-Perry formulation is shown once again: the non-linear elastic second-order "load-moment" path, shown by the dashed line, at one point intersects the cross-sectional failure surface - given by a straight line in the in-plane case. The level of axial force at this point is the buckling load of a column, while its normalized value (by a local, cross-sectional resistance "N$_L$") is the knock-down factor χ_y.

3 Derivation of the global buckling of beam-columns for the GSRM – monoaxial bending
The following derivation for beam-columns is first carried out only for the in-plane bending case and is based on and makes use of the same basic concepts as the Ayrton-Perry derivation for the column. Again, a linear cross-sectional failure criterion is used, in combination with a normalized representation of the "imperfection" of, in this case, of the load eccentricity represented by the bending moment. Initially discounting the imperfection effect (which will be reintroduced later), the bending moment eccentricity M/N can be normalized by the section core width. For the in-

plane case, for which the full derivation is shown in the following, this corresponds to the introduction of the following definition of η_y.

$$\eta_y = \frac{\frac{M_y}{W_y f_y}}{\frac{N}{A f_y}} \qquad (10)$$

Taking into account also the preceding step of the determination of the cross-sectional capacity, and *introducing the assumption that the linear failure surface of any surface can be described with sufficient accuracy (for the intended purpose) as being "parallel" to the elastic, first-yield failure surface*, the compression resistance and the bending moment resistance in y (in-plane bending) are a function of χ_L (see *Toffolon and Taras 2019*):

$$N_L = \chi_L A f_y \; ; M_{y,L} = \chi_L W_{y,el} f_y \qquad (11)$$

and η_y can be rewritten as:

$$\eta_y = \frac{\frac{M_y}{M_{y,L}}}{\frac{N}{N_L}} \qquad (12)$$

Fig. 2 shows that the behaviour of a beam-column member on global buckling is comparable to the column buckling behaviour with imperfections by using the relative eccentricity η_y.
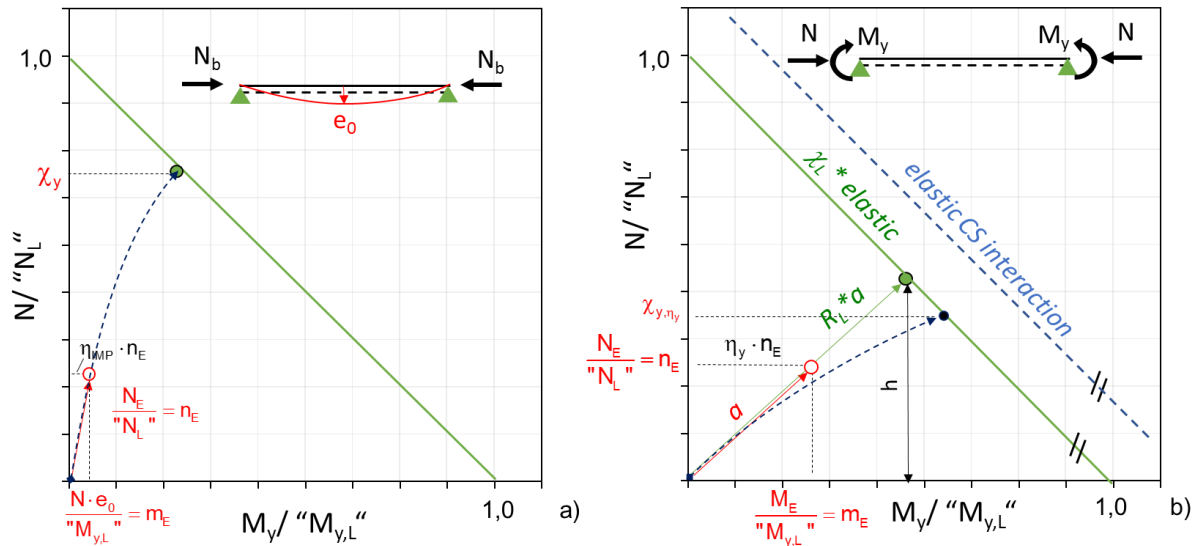

Fig. 2. Equivalence of an imperfection effect in a column (a) and bending effect in a beam-column (b).

In Fig. 2 b) the beam-column behaviour for in-plane bending is represented in terms of normalized bending moment m_y and normalized compression n, i.e.:

$$m_y = \frac{M_y}{M_L} \qquad (13)$$

$$n = \frac{N}{N_L} \tag{14}$$

In the same format the normalized applied loads are expressed as:

$$m_{y,E} = \frac{M_{y,E}}{M_L} \tag{15}$$

$$n_E = \frac{N_E}{N_L} \tag{16}$$

The green point in the figure represents the intersection of the proportionally amplified load vector of length "a" with the linear-elastic cross-section interaction multiplied by χ_L. The vector from the origin to this point has the length $R_L a$, where a is the length of the vector with components n_E and $m_{y,E}$. From the definition of h as the projection in the n axis of $R_L a$ it follows:

$$h = R_L n_E = 1 - R_L m_{y,E} \tag{17}$$

Then, solving this equation for R_L yields:

$$R_L = \frac{1}{n_E(1+m_{y,E}/n_E)} = \frac{1}{n_E(1+\eta_y)} \tag{18}$$

By defining $c_0 = (1 + \eta_y)$ in the equation it follows that

$$R_L = \frac{1}{n_E c_0} \tag{19}$$

In the formulation of the critical load R_{cr} of a RHS / SHS member failing in flexural buckling the effects of lateral torsional buckling can be neglected. It follows

$$R_L = \frac{N_{cr}}{N_E} \tag{20}$$

The aforementioned relative slenderness $\bar{\lambda}_y$ is a function of N_{cr} and the plastic resistance $N_{pl} = A f_y$. A new definition of relative slenderness $\bar{\lambda}_y{}^*$ is introduced as a function of N_L

$$\bar{\lambda}_y{}^* = \sqrt{\frac{N_L}{N_{cr,y}}} = \sqrt{\frac{\chi_L A f_y}{N_{cr,y}}} \tag{21}$$

The GSRM framework provides a more generalised definition of the relative slenderness $\bar{\lambda}_G$ for global buckling:

$$\bar{\lambda}_G = \sqrt{\frac{R_L}{R_{cr}}} \tag{22}$$

Where R_L is the cross-section capacity and R_{cr} is the critical load for flexural buckling. R_{cr} includes more than one global buckling mode in y and z direction, but the rules for global buckling

are here derived for the in-plane bending case, i.e. the mode referred to as FB$_{y-y}$ (see Fig. 5 for a graphic representation).

R_{cr} can thus be rewritten as

$$R_{cr} = \frac{N_{cr}}{N_E} = \frac{N_{cr}/N_L}{N_E/N_L} = \frac{1}{n_E \bar{\lambda}_y^{*2}} \tag{23}$$

By introducing $\bar{\lambda}_y^*$ in the $\bar{\lambda}_G$ definition and after few algebraic steps we obtain

$$\bar{\lambda}_G = \frac{\bar{\lambda}_y^*}{\sqrt{c_0}} \tag{24}$$

The definition of the global buckling resistance $R_{b,G}$ in the GSRM is as follows:

$$\chi_G = \frac{R_{b,G}}{R_L} \tag{25}$$

Where $R_{b,G}$ is the global buckling resistance and R_L is the cross-section resistance.

χ_{y,η_y} is the buckling reduction factor for the axial force (compression) component of the cross-sectional strength obtained by the Ayrton-Perry formulation, which considers again the non-linear elastic second-order load path displayed in Fig. 2 b).

$$\chi_{y,\eta_y} = \frac{N_b}{N_L} \tag{26}$$

It follows then

$$\chi_G = \frac{R_{b,G}}{R_L} = \chi_{y,\eta_y} c_0 \tag{27}$$

The derivation of the global buckling formulae for the GSRM starts with the derivation of χ_{y,η_y}, and is similar to the derivation of $\chi_{y,EC3}$. The limit-state equation in the quadratic format substituting $A f_y$ with N_L and $W_y f_y$ yields:

$$\frac{N_b}{N_L} + \frac{(M_b^I + N_b e_0)}{W_y f_y} \cdot \frac{1}{1 - N_b/N_{cr}} = 1.0 \tag{28}$$

Where $M_{y,b}^I = N_b \eta_y$.

After few algebraic steps and by introducing $\bar{\lambda}_y^{*2}$ and $\eta_{imp} = \frac{N_L e_0}{M_{y,L}}$

$$\chi_{y,\eta_y} + \left(\eta_{imp} + \eta_y\right) \cdot \frac{\chi_{y,\eta_y}}{1 - \chi_{y,\eta_y} \bar{\lambda}_y^{*2}} = 1.0 \tag{29}$$

Which is again a quadratic equation with the well-known solution

$$\chi_{y,\eta_y} = \frac{1}{\Phi + \sqrt{\Phi^2 - \bar{\lambda}_y^{*2}}} \tag{30}$$

$$\Phi = 0.5\left(1 + \left(\eta_{imp} + \eta_y\right) + \bar{\lambda}_y^{*2}\right) \tag{31}$$

Substituting the GSRM based variables $\bar{\lambda}_G = \frac{\bar{\lambda}_y^*}{\sqrt{c_0}}$ and $\chi_G = \frac{R_{b,G}}{R_L}$ we obtain

$$\chi_G = \frac{1}{\Phi_G + \sqrt{\Phi_G^2 - \beta_{LG}\bar{\lambda}_G^2}} \tag{32}$$

$$\Phi_G = 0.5\left(\beta_{LG}\left(1 + \eta_{imp} + \eta_y\right) + \bar{\lambda}_G^2\right) \tag{33}$$

With $\beta_{LG} = \frac{1}{c_0}$ \hfill (34)

and, once again, a substitution of the original term for η_{imp} with the expression calibrated by Rondal & Maquoi for the European column buckling curves

$$\eta_{imp} = \alpha_{EC3}\left(\bar{\lambda}_G\sqrt{c_0} - 0.2\right) \tag{35}$$

Thus, α_{EC3} is the value according to the EN 1993-1-1 buckling curves.
An overview of the shape of thus-obtained GSRM global buckling curves is given in Fig. 3, where the relative position of the buckling curve decreases with increasing η_y values.
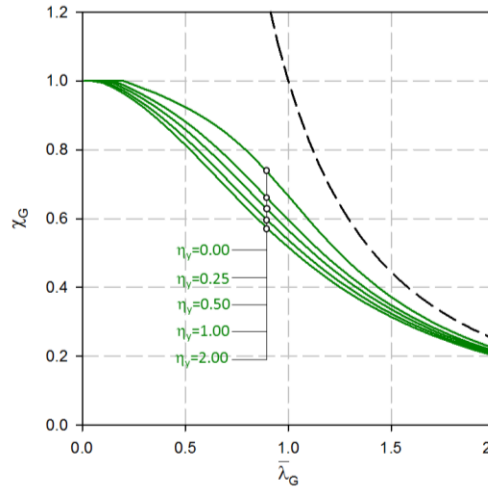

Fig. 3. In the figure an overview of the global buckling curves varying η_y is given.

4 Introduction of calibration factors and expansion to bi-axial loading

The derivation provided so far only accounts for an elastic behaviour, with geometric non-linearities account for only for as long as they are small, and material non-linearities included only partially and with unreliable accuracy, through the chosen cross-sectional resistance surface. In particular, the derivation does not include effects caused by the deterioration of stiffness once yielding sets on in the outermost fibres. Accordingly, in order to account for the typical effects of

the RHS and SHS cross-sections, additional parameters were added in the GSRM framework. This is relevant and necessary for all sections that reach a higher cross-sectional capacity than the one given by a first-yield criterion, i.e. for all cases where $\chi_L > 1$. Thus, a new term ξ_{LG} was introduced to account for the effects of the cross-section in the plastic range ($\chi_L > 1$). It can be interpreted as a reduction of the originally valid cross-sectional capacity surface, leading to the use of a new, "transition" surface for these cases. The procedure is schematically shown in Fig. 4 for the in-plane beam-column buckling case. As can be seen in the figure, the linear approximation of the cross-sectional resistance (represented by "N$_L$" and "M$_L$", as well as χ_L) is reduced to a new transition surface, so that in the original space the limit for the achievable axial force is now given by N/"N$_L$" = $1/\xi_{LG}$.
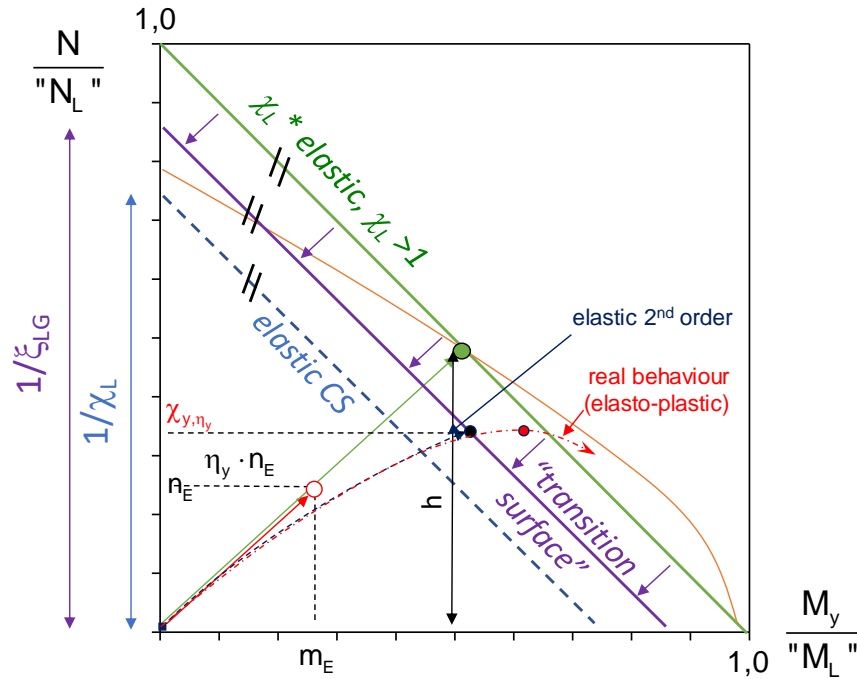

Fig. 4. Representation of the "transitional behavior" for beam-columns with elasto-plastic, stocky sections

The numerical parametric study has shown that it is indeed necessary to account for this effect in stocky sections. For the representation of the transition behavior it was chosen to define the term ξ_{LG} as a linear function of the generalised global slenderness $\bar{\lambda}_G$, with an additional factor ρ to act as a calibration factor for different types of section.
The chosen format for ξ_{LG} is thus:

$$1.0 \leq \xi_{LG} = 1 + (\chi_L - 1)\rho\bar{\lambda}_G \leq \chi_L \tag{36}$$

For RHS / SHS, it was found that the effect could be limited to a transition from the plastic range to the elastic range; this is represented by limiting ξ_{LG} by χ_L.
With the added term ξ_{LG}, the quadratic equation of the Ayrton-Perry derivation is modified as follows:

$$\xi_{LG}\chi_{y,\eta_0} + (\eta_{imp} + \eta_y) \cdot \frac{\xi_{LG}\chi_{y,\eta_0}}{1 - \chi_{y,\eta_0}\bar{\lambda}_y^2} = 1.0 \tag{37}$$

9

Which once again results in the aforementioned solution:

$$\chi_G = \frac{1}{\Phi_G + \sqrt{\Phi_G^2 - \beta_{LG}\bar{\lambda}_G^2}} \tag{38}$$

$$\Phi_G = 0,5 \cdot \left(\beta_{LG}\left(1 + \eta_{imp} + \eta_y\right) + \bar{\lambda}_G^2\right) \tag{39}$$

yet with a modified value of $\beta_{LG} = \frac{\xi_{LG}}{c_0}$

An expansion to the *spatial loading case,* i.e. for compression and bi-axial bending, is possible in a very straight-forward manner in the case of hollow-sections, since generally no torsional buckling phenomena occur in RHS and SHS beam-columns. In these, two paths of buckling are considered as possible buckling modes, corresponding to the two axes of bending, see Fig. 2. The "in-plane" case treated in the previous section is one of the two possible paths for flexural buckling and is defined as $FB_{y,y}$ for bending about the major axis. The equation is only modified to account for the simultaneous presence of a weak-axis bending moment. Similarly, the basic equation (i.e. the failure criterion) for the out-of-plane buckling case is very similar to the in-plane case, provided that the out-of-plane (weak-axis) flexural buckling slenderness is considered. The limit state equation is as follows:

$$\xi_{LG}\chi_{z,\eta_0} + \left(\eta_{imp} + \eta_z\right) \cdot \frac{\xi_{LG}\chi_{z,\eta_0}}{1 - \chi_{z,\eta_0}\bar{\lambda}_z^2} + \xi_{LG}\eta_y\chi_{z,\eta_0} = 1.0 \tag{40}$$
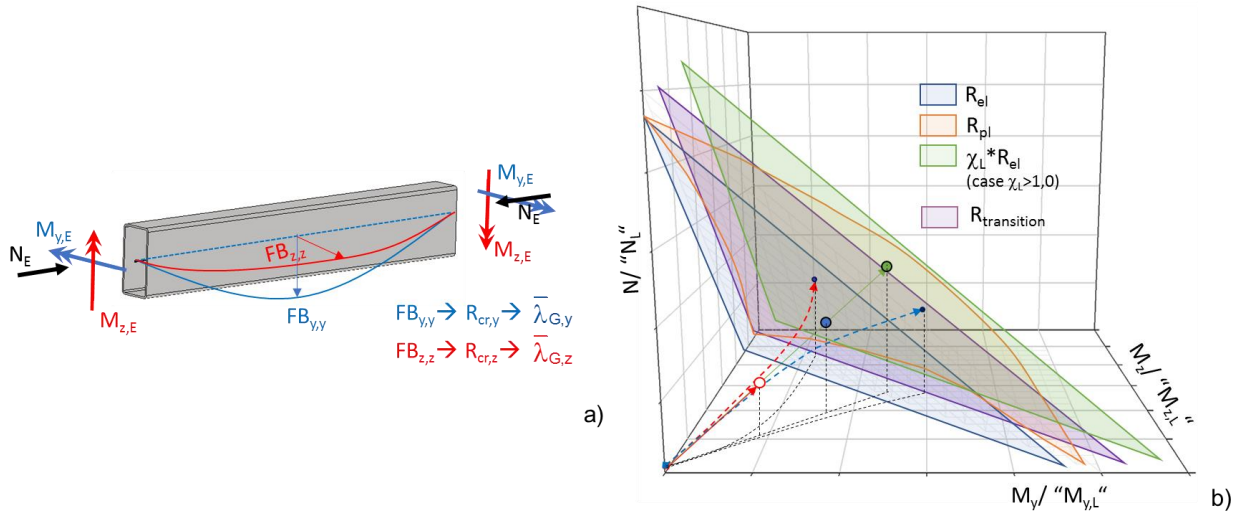

Fig. 5. Spatial case; loading and slenderness definitions (a); limit surfaces and possible load paths (b).

5 Examples of the calibration accuracy

In the following pages, examples are given of the accuracy of the chosen calibration factors for the proposed Ayrton-Perry formulation for overall, global buckling of RHS/SHS beam-columns. This is first done using the representation of the results in the $\bar{\lambda}_G - \chi_G$ plot. Thereby, the knock-down factor is represented by:

$$\chi_G = \frac{R_{GMNIA}}{R_{EL}\chi_L} \tag{41}$$

while the slenderness is given by the following definition, as previously established:

$$\bar{\lambda}_G = \sqrt{\frac{R_{EL}\chi_L}{R_{cr,G}}} \tag{42}$$

As is illustrated in the following Fig. 6, the behaviour of the GMNIA results is consistently described by the GSRM formulation. The left-sided part a) of this figure shows a class 1 SHS subjected to in-plane loading, with three different eccentricity levels and a uniform bending moment diagram. The points represent the GMNIA results while the curve shows the corresponding buckling curve according to the developed and calibrated GSRM. In sub-plot b), similar results for a class 3 SHS subjected to in-plane loading are shown. Quite generally, For the in-plane case, the combined accuracy of χ_G and χ_L generally leads to quite precise results. The conservatism is more pronounced for cold-formed sections, where EC3 imposes $\alpha_{EC3} = 0.49$.
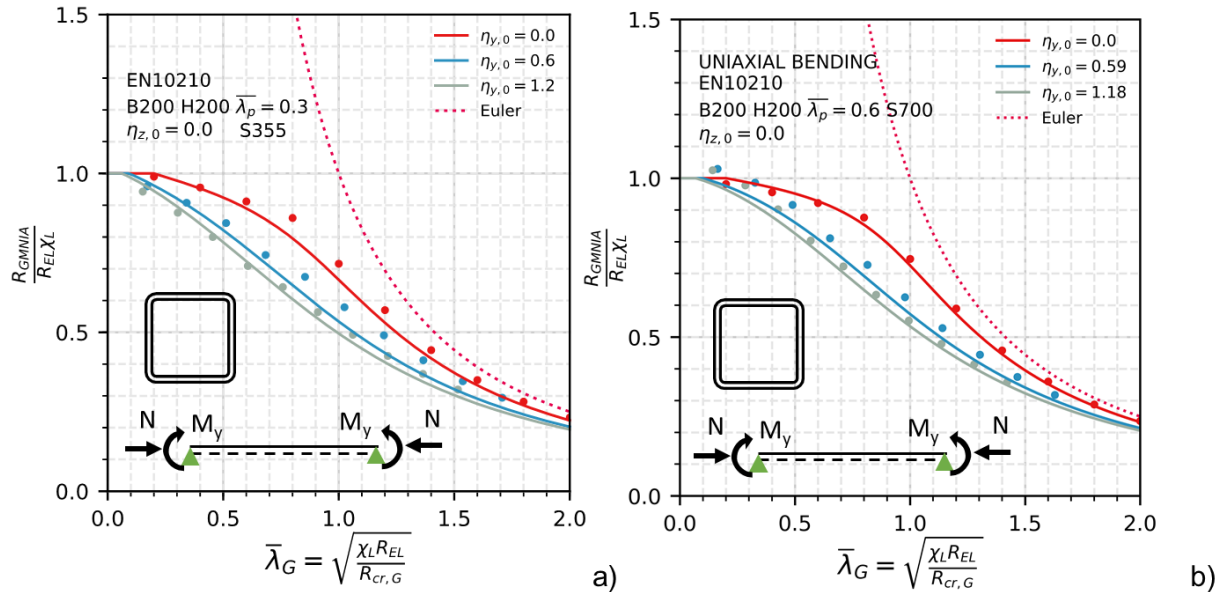

Fig. 6. Comparison of GMNIA results (dots) and calibrated GSRM predictions (continuous lines) for various levels of eccentricity and hot-finished SHS with various plate thickness values; a) plate slenderness $\bar{\lambda}_p$=0.3 (class 1 section); b) $\bar{\lambda}_p$=0.6 (class 3 section)

Through calibration and the selection of satisfactorily safe and accurate strength predictions, the following values of ρ were selected:

- $\rho = 0.6$ for hot-finished section
- $\rho = 0.5$ cold-formed sections

The calibration of the GSRM parameters also produced accurate and satisfactorily safe-sided results for RHS, both for the in-plane and out-of-plane cases. A few exemplary cases are illustrated in Fig. 7. In sub-plot b), the effect of the local buckling conservatism is eliminated from the representation by using a slightly different format of χ_G:

$$\chi_G = \frac{R_{GMNIA}}{R_{GMNIA,SHORT}} \tag{43}$$

In this case, the value of the each GMNIA result is divided by the value of the shortest member of the corresponding load case, and it can be noticed that the rather high conservatism of the GSRM predictions of the value in the global case of Fig. 7 a) is mostly due to the predicted value of the cross-section capacity, which happens to be quite conservative (by around 20%) for this particular cross-section.
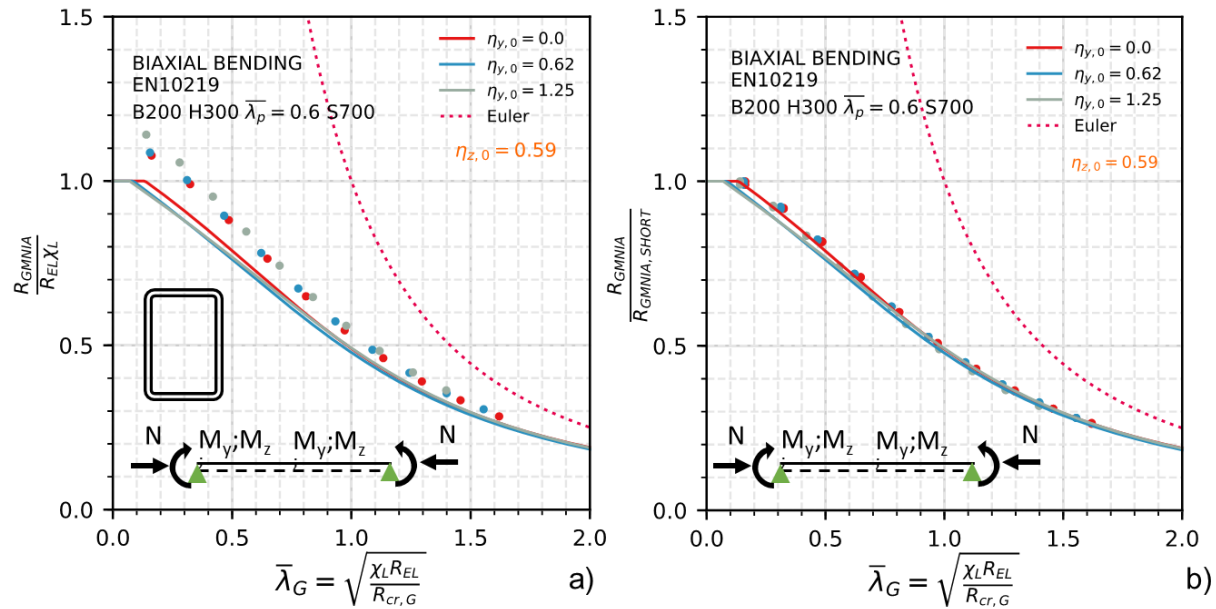

Fig. 7. Class 3-4 RHS subjected to biaxial bending. In a) the traditional representation of the GMNIA results in the GSRM format is shown; b) shows the results without the effects of the cross-section conservatism of χ_L.

Finally, the last parameter that needed to be introduced for a more general implementation of the method accounts for the cases where the bending moment is not constant along the member length. In the extensive parametric study several combinations of the bending moment diagrams along the member length were applied, and a bending moment factor C_m was introduced, in correspondence with the common use in Eurocode 3. This is shown by example in the following.

In Fig. 8a), the GMNIA results for the application of an exemplary non-constant, linear bending moment diagram are plotted in the GSRM format. In an attempt to diverge as little as possible

from established EC3 design rules, the existing formulae and tables for C_m were adapted, leading to the use of $C_{m,y} = 0.6$ for this particular case. A schematic overview of the resulting accuracy for an SHS section and various levels of bending is given in the figure. Fig. 8 b) contains the proposed values for some simple bending moment cases.
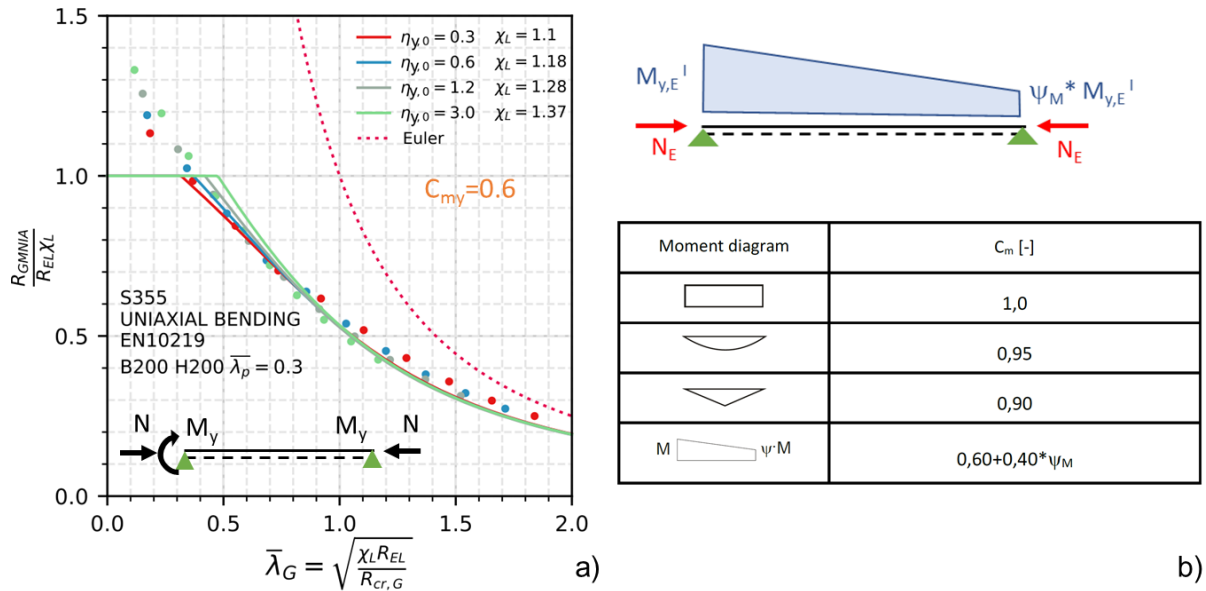

Fig. 8. In a) class 1 SHS subjected to in-plane linear bending moment over the length; in b) an overview of the evaluated applied bending moment and a schematic representation of the ψ_M factor.

Thus, the final version of the global buckling calibrated formulation includes coefficients $C_{m,y}$ and $C_{m,z}$ to account for the effects of the different bending moment diagrams in both directions. They enter the formulae by directly reducing the maximum value of the bending moment along the member. Thus, the parameters $C_{m,y}$ and $C_{m,z}$ are multiplied respectively to η_y and η_z.

6   Overall validation against GMNIA results and comparison with AISC and Eurocode 3

An overview of the results of the parametric study is necessary in order to validate the GSRM formulation with respect to accuracy and safety, as well as to compare the efficiency of the method with the current design standard. Thereby, the GSRM rules, which were calibrated against the data pool of the extensive parametric study, are now validated against the EC3 and AISC design values. A much larger set of points is used in the following, representative results, which will be grouped for members of equal flexural buckling slenderness $\bar{\lambda}_z$, where:

$$\bar{\lambda}_z = \sqrt{\frac{Af_y}{N_{cr,z}}} \tag{44}$$

The chosen representation format is the so-called box plot format, which allows a graphical evaluation of the statistical parameters in the plot. A box in red color is used to represent the area

that contains 50% of the data for a certain slenderness, while the whiskers show the 5% upper and lower bound of the data, and the "outliers" beyond this range are shown as small black points. Fig. 9 shows predicted values from numerical simulations with constant bending moment along the member length and compression, uni- and biaxial bending. In Fig. 9 a) and b), the results of the GMNIA numerical campaign on global buckling are normalized by the strength prediction of the new GSRM formulation. The corresponding scatter bands are shown for a) hot-finished steel sections (*EN10210*) and b) cold-formed steel sections (*EN10219*). The scatter is higher for cold-formed sections, reaching consistently about the same resistance of the GSRM prediction with the 5% lower bound and 25% higher results with the 5% upper bound. Hot-finished sections instead behave differently on the upper bound of the result distribution, with a maximum of 20% of higher resistance for $\bar{\lambda}_z$=1,2. in Fig. 9 c) and d) gives a representation similar to a) and b); each GMNIA simulation is divided respectively by the EC3 and AISC design value.

In general, the GMNIA results are fairly above the EC3 predictions except few points located in low slenderness rang, where also the effect of the cross-section capacity is higher and the prediction of the Eurocode could be occasionally unsafe (e.g. *Toffolon and Taras 2019b*). In Fig. 9 d) the GMNIA results are divided against the AISC design values. The scatter of the values is higher that the Eurocode, and this is more noticeable for high slendernesses. The predictions for $\bar{\lambda}_z$=1,0-1,5 lie well below the average GMNIA value, in some cases with a median AISC design value more than 10% lower than the GMNIA. In Fig. 9 e) and f) show equivalent results by comparing directly the AISC design rules with the Eurocode and the GSRM. In the comparison, the predictions of the AISC are on average 20% higher than the corresponding values from the European standard, and still 13% higher compared to the GSRM predicted values. As shown in Toffolon and Taras 2019b, the safety factor proposed for the GSRM method is 1.0, while the AISC rules would require a lowering of all values by LRFD resistance factors, thus bringing down the average design resistances to the level of the GSRM predictions.

For an overview of the mean values and standard deviation of the proposed comparisons, see Table 2.

Table 2. Statistical evaluation of the parametric study on global buckling.

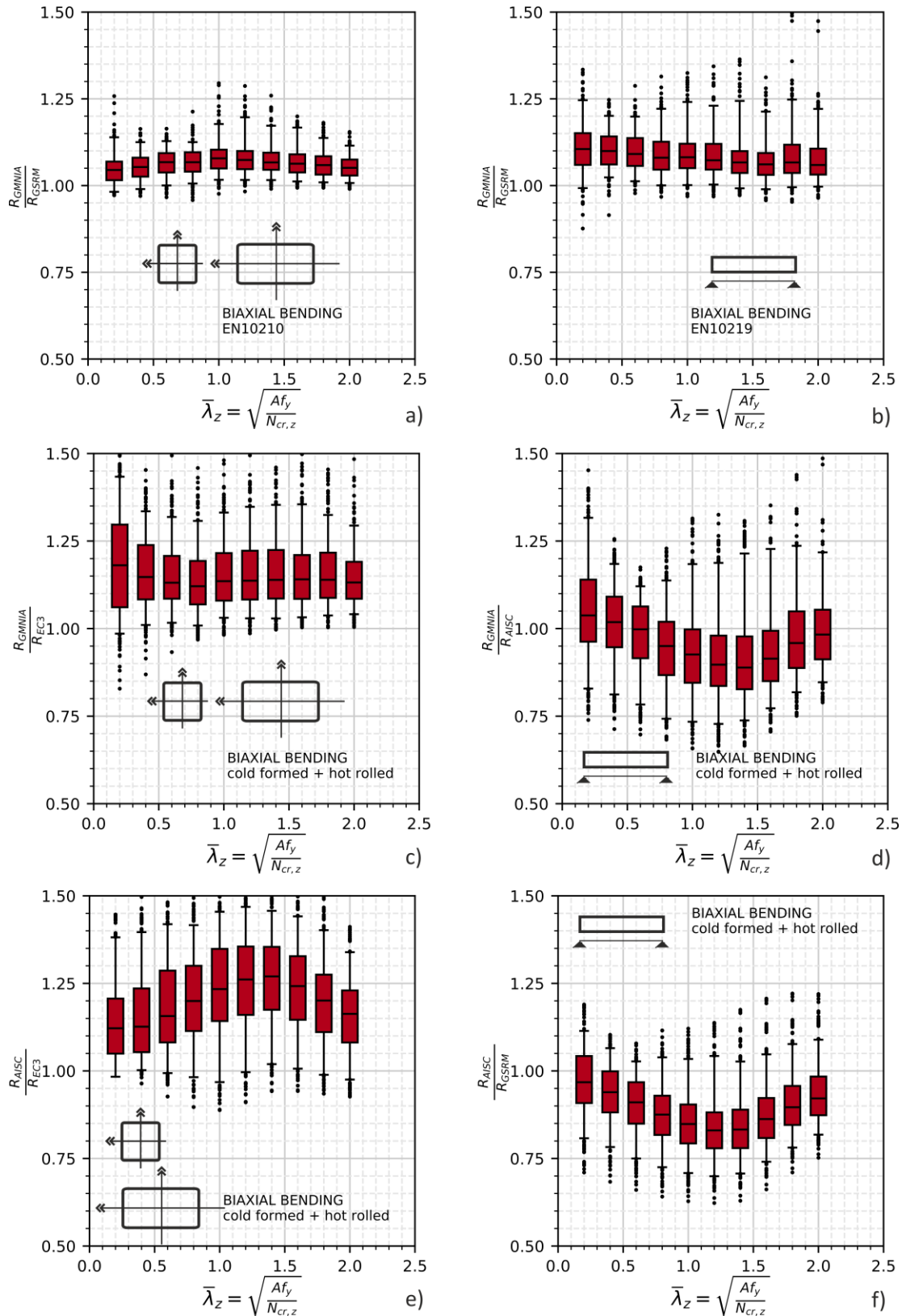| Plot	Mean	Standard deviation
Fig. 9 a	1.067	0.051
Fig. 9 b	1.092	0.074
Fig. 9 c	1.157	0.103
Fig. 9 d	0.968	0.134
Fig. 9 e	1.201	0.135
Fig. 9 f	1.131	0.127

Fig. 9. Comparison of results through box plots; a) and b): GMNIA vs. GSRM, hot-finished and cold-formed steel; c) GMNIA vs. EC3 rules; d) GMNIA vs. AISC rules; e) and f): AISC vs. EC3 and AISC vs. GSRM rules.

7   Summary and Conclusions

This paper describes and provides the background to a new design method for the determination of the strength of SHS and RHS beam-column members made of mild or high-strength steel and loaded by any combination of axial (compressive) forces and bending moments about one or both principal axes of rotation. The new method, termed the Generalized Slenderness-based Resistance Method (GSRM), makes use of a generalization of the slenderness values at a local and global level, which are commonly determined with the aid of dedicated numerical tools. When applied to beam-columns, the GSRM calculates - in a first step - the design value for the cross-section resistance and applies – in a second step - an Ayrton-Perry-type formulation for the design of members. Thereby, the generalized slenderness and the cross-section resistance are the main inputs. This formulation for beam-columns was calibrated against a large pool of numerical results, accounting not only for the second order effects at a global level, but also for the spread of plasticity for stocky cross-sections and general load cases (combined compression and biaxial bending). These results expand the GSRM rules for the cross-section resistance developed during the HOLLOSSTAB project and may be applied to various types and shapes of hollow sections. In this paper, the results of the GSR method are compared with well-known American and the European code predictions for the cross-section resistance, demonstrating significant improvements in consistency, safety and cross-section strength. In addition, the research project HOLLOSSTAB also led to the development of a second, strain-based (CSM) approach (*Meng et al. 2019*) for the design of stockier cross-sections as well as the GSRM design rules for the global buckling of members. The full mechanical background to development of GSRM formulations for the design of members can be found in *Taras et al. (2019)* and is in the process of publication in journal papers.

References

AISI S100-16 (2016), North American Specification for the Design of Cold-Formed Steel Structural Members, American Iron and Steel Institute

ANSI/AISC 360-16 (2016), Specification for Structural Steel Buildings, American Institute of Steel Construction, Chicago IL.

Ayrton, W. E., Perry, J. (1886). On Struts, The Engineer, 62, London, pp.464-465, 513-515.

Bjorhovde, R. (1972), Deterministic and Probabilistic Approaches to the Strength of Steel Columns, PhD Dissertation, Lehigh University, Bethlehem, PA.

Bjorhovde, R. (1992), Compression Members, *Constructional Steel Design: An International Guide*, ed. P.J. Dowling, J.E. Harding, Elsevier Applied Science, London, pp.67-90.

EN 10219 (2006): Cold formed welded structural hollow sections of non-alloy and fine grain steels, CEN – European Committee for Standardization, Brussels.

EN 10210 (2006): Hot finished structural hollow sections of non-alloy and fine grain steels, CEN – European Committee for Standardization, Brussels.

Eurocode 3 (2006): Design of steel structures - Part 1-5: General rules - Plated structural elements, CEN - European Committee for Standardization, Brussels, version EN 1993-1-5.

Eurocode 3: (2018) Design of steel structures – Part 1-1: General rules and rules for buildings, CEN - European Committee for Standardization, Brussels, Draft standard under review by National Standardisation Bodies, version prEN 1993-1-1.

Galambos, T. V. (1998): *Guide to Stability Design Criteria for Metal Structures*, 5th Edition, Wiley, Boston.

Meng, X.; Toffolon, A.; Gardner, L.; Taras, A. (2019): The generalized slenderness-based resistance method for design of CHS and EHS, *Steel Construction*, 12-4, pp.342-353.

Robertson, A. (1925). The Strength of Struts, *The Institution of Civil Engineers – Selected, Engineering Papers*, 28, London.

Rondal, J., Maquoi, R. (1979). Formulations d'Ayrton-Perry pour le Flambement des Barres Métalliques, *Construction Metallique*, No. 4, pp.41-53.

Taras, A.; Toffolon, A.; Gardner, L.; Meng, X. (2019b): Background on the development of Overall-Slenderness based design rules for RHS and SHS, *HOLLOSSTAB, RFCS Grant Nr. 2015-709892, Deliverable 8.2*, Munich.

Toffolon, A.; Taras, A. (2019a): Development of an OIC-Type local buckling design approach for cold-formed unstiffened and groove-stiffened hollow sections, *Thin-Walled Structures*, 144.

Toffolon, A., Taras, A., Meng, X., Gardner, L. (2019b): The generalized slenderness-based resistance method for design of RHS and SHS, *Steel Construction*, 12-4, pp.327-341.

Ziemian, R. D. (2010): *Guide to Stability Design Criteria for Metal Structures*, 6th Edition, Wiley, Boston.